

SilentWood: Private Inference Over Gradient-Boosting Decision Forests

Ronny Ko
LG Electronics
Seoul, South Korea
hajoon.ko@lge.com

Rasoul Akhavan Mahdavi
University of Waterloo
Canada
r5akhava@uwaterloo.ca

Byoungwoo Yoon
LG Electronics
South Korea
byoungwoo.yoon@lge.com

Makoto Onizuka
Osaka University
Japan
onizuka@ist.osaka-u.ac.jp

Florian Kerschbaum
University of Waterloo
Canada
fkerschb@uwaterloo.ca

Abstract—Gradient-boosting decision forests, as used by algorithms such as XGBoost or AdaBoost, offer higher accuracy and lower training times for large datasets than decision trees. Protocols for private inference over decision trees can be used to preserve the privacy of the input data as well as the privacy of the trees. However, naively extending private inference over decision trees to private inference over decision forests by replicating the protocols leads to impractical running times. In this paper, we explore extending the private decision inference protocol using homomorphic encryption by Mahdavi et al. (CCS 2023) to decision forests. We present several optimizations that identify and then remove (approximate) duplication between the trees in a forest and hence achieve significant improvements in communication and computation cost over the naive approach. To the best of our knowledge, we present the first private inference protocol for highly scalable gradient-boosting decision forests. Our optimizations extend beyond Mahdavi et al.’s protocol to various private inference protocols for gradient-boosting decision trees. Our protocol’s (SilentWood) inference time is faster than the baseline of parallel running the protocol by Mahdavi et al. by up to 28.1x, and faster than Zama’s Concrete ML [1] XGBoost by up to 122.25x.

1. Introduction

Machine Learning as a Service (MLaaS) allows large user groups to use machine learning models. A service provider trains a model and offers users inference using this model. One common such example is ChatGPT. An advantage of this model is that the provider can control access to the model and easily update it when new training data is available. In contrast, its disadvantage is the privacy concern of the users revealing their sample data to the provider which may be sensitive or legally restricted. Cryptography offers a compelling solution to this problem. The user can encrypt its data, e.g., using fully homomorphic encryption [2], [3], and the provider can perform private inference. However, this solution usually has high computational costs. Alternatively, the user and the

provider can engage in a two-party computation [4], [5], [6] which has, however, usually higher communication costs. Using this private inference, the provider still hosts the model, but the user’s privacy objectives are met.

In this paper, we develop a new protocol for private inference over gradient-boosting decision forests. Gradient-boosting decision forests are collections of decision trees whose results are combined into the final model prediction. The advantage of gradient-boosting forests is that they offer a better trade-off between higher accuracy and lower training time than training a single decision tree for large datasets. Moreover, they retain a critical advantage of decision trees over many other machine learning techniques; their predictions can be easily explained helping to fulfill legal, social, and ethical requirements.

Many private inference protocols over decision trees exist, e.g., [7], [8], [9], [10], [11], [12], [13], [14], [15], [16], [17], [18], [19], [20], [21], [22], [23]. However, extending these to gradient-boosting decision forests comes with two complications. First, the results of the decision trees need to be combined into a single prediction result requiring further computation. This can particularly pose a problem for protocols using homomorphic encryption [10], [11], [20], [21], [22], [23], since these computations increase the multiplicative depth of the circuit and hence require larger parameters significantly increasing the resource requirements by the protocols. Second, even just naively running several, independent decision tree protocols without combining their results can exhaust current computing resources. Therefore, optimizations are necessary that reduce the cost of executing multiple decision tree evaluations on the same input.

Although most of our contributions are independent of the specific decision tree private inference protocol used and are also applicable to many other protocols using homomorphic encryption, we extend the protocol by Mahdavi et al. [20] to gradient-boosting decision forest evaluation, to exemplify our advances. This protocol is state-of-the-art in private inference over decision trees using homomorphic encryption. We value its low communication cost and are able to preserve it in our extension which provides a compelling advantage over two-

party computations. However, naively repeating this protocol to all decision trees (100 in our default setup), computing the final score can take more than 5 minutes, which is prohibitive for many applications. The inference time of SilentWood is faster than this baseline by up to 28.1x, and faster than Zama’s Concrete ML [1] XGBoost by up to 122.25x.

Our new protocol design contributes the following:

- We develop a new blind code conversion protocol for our inference which converts between different encodings of indicator bits used in decision protocols. We provide a detailed security analysis and report on its computation and communication cost. See §4.1.
- We develop two optimizations that identify and remove (approximate) duplications between the trees in a forest and hence significantly reduce the overall complexity. We report on the computation and communication improvements and the accuracy impact of these optimizations. See Section 4.2.
- We develop optimization that identify and remove duplications between the inputs to a decision forest and significantly reduce communication size. We report on the communication improvements and its overall impact on the computation cost. See Section 4.3.

The remainder of the paper is organized as follows. In Section 2 we introduce gradient boosting models and fully homomorphic encryption. We describe the previous work we improve over in Section 3. In Section 4 we present the details of our protocol SilentWood. We report on our implementation and evaluation results in Section 5 and summarize related work in Section 6. We conclude the paper with our findings in Section 7.

2. Background

2.1. Gradient Boosting Models

Ensemble decision trees [24] is a machine learning technique that combines multiple small trees as weak learners to improve overall prediction. There are two types of ensemble methods: random forests [25] and gradient boosting [26]. Random forests build multiple trees independently and make the final prediction by aggregating the predictions from individual trees (e.g., voting or averaging). Gradient boosting also builds multiple trees, but sequentially, to incrementally correct the errors of the previous ones and collectively build a strong model through incremental improvement. XGBoost [27] and AdaBoost [28] are among the most widely used gradient boosting algorithms. In this work, we focus on private inference of these two boosted decision tree models.

In AdaBoost, each trained tree is assigned a weight, and each leaf node is assigned a sign, where ‘+’ and ‘-’ correspond to binary classes. The inference procedure is as follows: (1) traverse each tree from the root node by comparing the client’s feature input values with the threshold values at each node; (2) reach and retrieve the leaf node’s value; (3) multiply it by the weight assigned to its tree; (4) sum all such intermediate values computed from all trees; and (5) determine the sign (+/-) of the final summed value as the inferred binary class.

XGBoost supports both binary and multi-class classification. For binary classification, we sum the leaf node values of all traversed trees, apply the sigmoid function to this sum, and then determine the binary class based on whether the computed sigmoid value is greater than 0.5. For multi-class classification, we sum the leaf node values of all traversed trees corresponding to each class, obtaining a summed value for each class. We then apply the softmax function to these summed results and determine the class with the maximum softmax value as the inferred class.

2.2. Fully Homomorphic Encryption

Fully Homomorphic Encryption (FHE) [29] is a cryptographic scheme that allows addition or multiplication of plaintexts encrypted within ciphertexts without decrypting them. Among various FHE schemes, SilentWood uses an RLWE-family scheme (specifically BFV [30]) due to its efficient support for SIMD (Single Instruction Multiple Data) operations. In this scheme, the granularity of operation is a vector of elements, where each element is a plaintext value. To use the RLWE-family scheme, we first encode (**Encode**) the n -dimensional plaintext input vector into an $(n - 1)$ -degree polynomial $M(X)$, and then encrypt (**Encrypt**) the polynomial into an RLWE ciphertext using a secret key polynomial $S(X)$ as $\text{RLWE}_{S(X)}(M(X))$. Given such ciphertexts, we can perform cipher-plaintext addition (**PAdd**) between an RLWE ciphertext and a plaintext polynomial, cipher-cipher addition between two RLWE ciphertexts, cipher-plaintext multiplication, cipher-cipher multiplication, and rotation (in a round-robin manner) of the plaintext vector elements encrypted in a ciphertext, all without decrypting them. We summarize the FHE operations as follows:

- 1) **Encode** $([v_0, v_1, \dots, v_{n-1}]) \rightarrow M(X)$
- 2) **Decode** $(M(X)) \rightarrow [v_0, v_1, \dots, v_{n-1}]$
- 3) **Encrypt** $(M(X), S(X)) \rightarrow \text{RLWE}_{S(X)}(\Delta \cdot M(X))$
Δ is a big scaling factor (as part of the scheme)
- 4) **Decrypt** $(\text{RLWE}_{S(X)}(\Delta \cdot M(X)), S(X)) \rightarrow M(X)$
- 5) **PAdd** $(\text{RLWE}_{S(X)}(\Delta \cdot M_1(X)), M_2(X))$
 $\rightarrow \text{RLWE}_{S(X)}(\Delta \cdot (M_1(X) + M_2(X)))$
- 6) **CAdd** $(\text{RLWE}_{S(X)}(\Delta M_1(X)), \text{RLWE}_{S(X)}(\Delta M_2(X)))$
 $\rightarrow \text{RLWE}_{S(X)}(\Delta \cdot (M_1(X) + M_2(X)))$
- 7) **PMult** $(\text{RLWE}_{S(X)}(\Delta \cdot M_1(X)), M_2(X))$
 $\rightarrow \text{RLWE}_{S(X)}(\Delta \cdot (M_1(X) \cdot M_2(X)))$
- 8) **CMult** $(\text{RLWE}_{S(X)}(\Delta M_1(X)), \text{RLWE}_{S(X)}(\Delta M_2(X)))$
 $\rightarrow \text{RLWE}_{S(X)}(\Delta \cdot (M_1(X) \cdot M_2(X)))$
- 9) **Rotate** $(\text{RLWE}_{S(X)}(\Delta \cdot M(X)), r)$
 $\rightarrow \text{RLWE}_{S(X)}(\Delta \cdot M'(X))$, where
Decode $(M(X)) = [v_0, v_1, \dots, v_{n-1}]$ and
Decode $(M'(X)) = [v_r, v_{r+1}, \dots, v_0, v_1, \dots, v_{r-1}]$

One important benefit of RLWE-family schemes is that their homomorphic addition and multiplication support efficient SIMD operations over the underlying plaintext vector. Upon addition or multiplication of two RLWE ciphertexts, the underlying vectors in the ciphertexts are added or multiplied element-wise all at once. The same is true for cipher-plaintext computation: the encrypted vector in the RLWE ciphertext

and the encoded vector in the RLWE plaintext are added or multiplied element-wise.

In RLWE-family schemes, the typical dimension size of plaintext vectors is 2^{13} , 2^{14} , or 2^{15} , which is essentially the parallelism level of SIMD.

In this paper, we use the above eight FHE operations as black boxes to homomorphically compute the inference result of gradient boosting models.

3. RCC-PDTE by Mahdavi et al.

Private Decision Tree Evaluation (PDTE) is a protocol between a server and client. The client’s input is a vector of values representing a sample data point, and the server’s input is a gradient-boosting decision forest. At the end of the protocol, the server learns nothing about the client’s inputs, while the client learns nothing about the server’s model other than the prediction result and the model’s hyperparameters (e.g., types of features and classes). The set of classes is unknown to the client (due to the need to interpret the class’s meaning) and the client would usually pick the class with the highest probability as the prediction, although it can apply more sophisticated algorithms in case of near ties.

3.1. Greater-Than Comparison with FHE

Traversing a decision tree requires greater-than comparisons between the input features and the threshold at each tree node. However, as explained in §2.2, the only arithmetic operations supported by FHE is addition and multiplication ($+$, \cdot). Therefore, to homomorphically compare two numbers, a solution is to design an arithmetic logic circuit comprising only ($+$, \cdot) operations such that the gate returns 1 if $\alpha > \beta$, and returns false if $\alpha \leq \beta$.

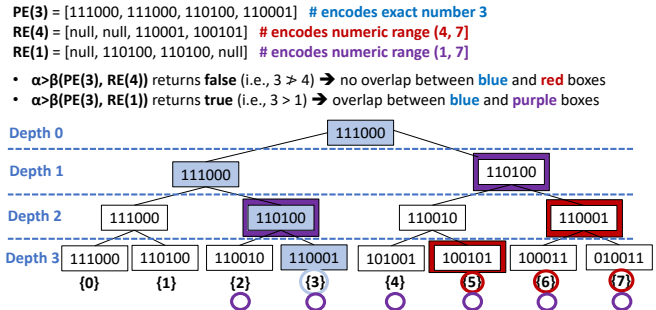


Figure 1: Examples of number comparison operations ($3 > 4?$ $3 > 1?$) where each node’s label is CW-encoded.

Figure 1 illustrates a high-level idea of how to compare two numbers by encoding each of them as a vector of node labels that form a complete binary tree (CBT, which is different from a decision tree), where each leaf node corresponds to the target number to encode. The CBT has 8 leaves and can encode any numbers between 0 and 7. Based on this CBT, RCC-PDTE proposes two number encoding schemes: PE (point encoding) and RE (range encoding). PE encodes an exact number corresponding to a particular leaf node of

We run this function at each tree node, where α = feature, β = threshold

```
bool alpha > beta(PE(alpha), RE(beta)): # Given PE(alpha) and RE(beta), determine if alpha > beta
int accumulator = 0;
for (int i = 0; i < PE(alpha).length; i++)
  accumulator += is_equal(PE(alpha)[i], RE(beta)[i])
return accumulator; # returns 1 if alpha > beta; 0 otherwise

bool is_equal(x, y) # returns 1 if x == y; 0 otherwise
int h = 0;
for (int i = 0; i < L; i++) # L: bit length of the encoded values
  h += x[i] * y[i]
m = 1;
for (int i = 0; i < H; i++) # H: Hamming weight (number of 1s)
  m *= h - i
int H_FACTORIAL = H*(H-1)*(H-2)*...*3*2*1 # a pre-computed constant
return (H_FACTORIAL)^-1 * m # where m is either H_FACTORIAL or 0
```

Figure 2: An arithmetic circuit of comparing two input numbers (α, β) encoded by CW-encoding ($\text{PE}(\alpha), \text{RE}(\beta)$).

CBT as a vector of node labels comprising the path from the root to a target leaf node. In Figure 1, we PE-encode 3 as PE vector [111000, 111000, 110100, 110001] (visualized as blue nodes and a blue circle). The CBT’s each node label is encoded as constant-weight encoding [31] (CW-encoding), which is essentially a Hamming-weight encoding whose base-2 representation always contains the same frequency of 1s for any target number to encode. We will later explain why we used CW-encoding for labeling.

Unlike PE encoding, RE encodes a range of numbers as a vector such that its each element corresponds to a specific node in each tree depth (or can be NULL not to choose any node), and the encoded range of numbers is the set of all descendant leaves of the nodes in the vector. In Figure 1, we RE-encode range (4, 7] as RE vector $\text{RE}(4) = [\text{null}, \text{null}, 110001, 100101]$ (visualized as red nodes), whose each element’s descendant leaves collectively cover number range {5, 6, 7} (red circle). As another example, we RE-encode range (1, 7] as $\text{RE}(1) = [\text{null}, 110100, 110100, \text{null}]$ (purple nodes), whose descendant leaves collectively cover number range {2, 3, 4, 5, 6, 7} (purple circles). Note that the upper bound of the range encoded by RE is always the right-most leaf value in CBT (e.g., 7 in case of Figure 1).

Based on this CBT setup, to evaluate the condition $\alpha > \beta$, we determine whether two vectors $\text{PE}(\alpha)$ and $\text{RE}(\beta)$ share any common node (i.e., same node label at the same depth of CBT). If yes, then $\alpha > \beta$ holds; otherwise $\alpha \leq \beta$. For example, $\text{PE}(3)$ and $\text{RE}(4)$ have no common node at any depth, which visually implies that the blue path of $\text{PE}(3)$ has no overlap with the red boundary of $\text{RE}(4)$ (i.e., $3 \leq 4$). On the other hand, $\text{PE}(3)$ and $\text{RE}(1)$ have a common node at depth 2 (110100), which visually implies that the blue path of $\text{PE}(3)$ has an overlap with the purple boundary of $\text{RE}(1)$ (i.e., $3 > 1$). This number comparison logic is implemented in the upper dashed box of Figure 2. Within this function, the for-loop statement can be executed with FHE as a series of ($+$, \cdot) operations, and we further detail the is_equal function’s internal logic in the lower dashed box, which again comprises only ($+$, \cdot) operations. Therefore, the entire number comparison operation can be performed by FHE with the target numbers being encrypted ciphertexts. In particular, is_equal assumes that the CBT’s each node label

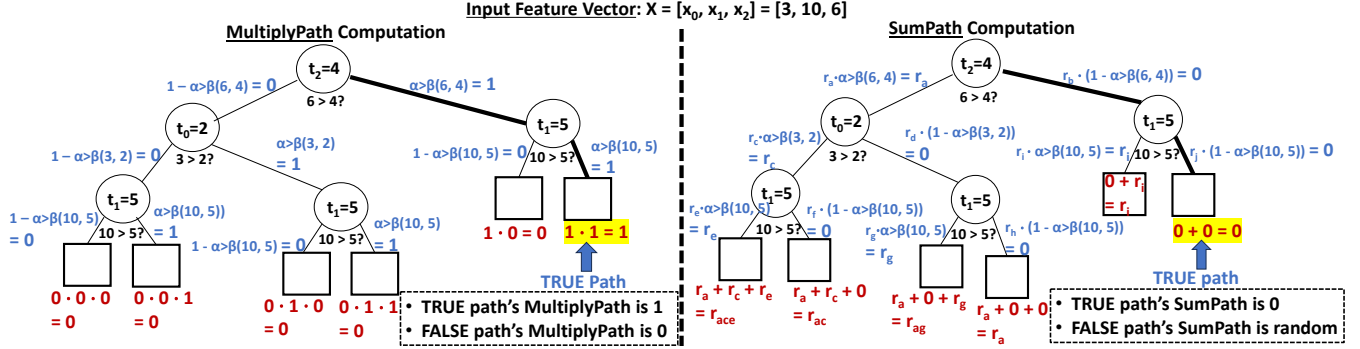


Figure 3: Computation of MultiplyPath and SumPath

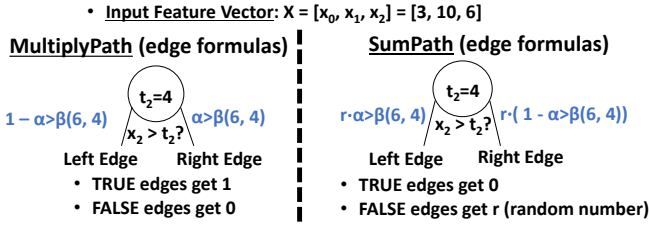


Figure 4: Edge formulas for SumPath and MultiplyPath

is encoded as CW-encoding. Note that all for-loops in these functions have a deterministic number of looping, because the conditional variables for looping (.length, L, and H) are statically known values. The benefit of using CW encoding in this comparison algorithm is that during the FHE computation, we can effectively fix the number of multiplicative depth (fixed to $\lceil \log H \rceil + 2$) required for the `is_equal` operation regardless of the bit-length of input data (x, y) .

3.2. Tree Path Computation

Now that we have homomorphically compared the thresholds and input features at each tree node, we use each node's (encrypted) comparison result to compute the path results. RCC-PDTE provides two ways to compute this: MultiplyPath (i.e., path conjugation) and SumPath [15]. Figure 4 depicts the left/right edge formulas for MultiplyPath and SumPath, each. The property of MultiplyPath edge formulas is that the condition-satisfying true edges get 1 and false edges get 0, whereas in case of the SumPath edge formulas the true edges get 0 and false edges get non-zero random numbers (r) . Based on these edge formulas, Figure 3 shows how to compute the final path values. In case of MultiplyPath, we compute each path's final value by multiplying all edge values that comprise the path. Therefore, the true path gets the final value 1, whereas all other false paths get the final value 0. On the other hand, in case of SumPath, we compute each path's final value by summing all edge values that comprise the path. Therefore, the true path gets the final value 0, whereas all other false paths get the final value of some non-zero random number. SumPath can be computed more efficiently by FHE, because it involves only addition operations, whereas MultiplyPath requires heavy multiplications whose frequency is as large as the length of each path.

Once all SumPath values are homomorphically computed, the server returns them back to the client, who decrypts them and considers the leaf value having SumPath 0 as the final classification result.

3.3. Limitations of RCC-PDTE

Although RCC-PDTE is the state-of-the-art FHE-based PDTE algorithm, when it comes to evaluation of decision forests, there occurs three problems:

Problem 1: Aggregating the Final Score. For XGBoost inference, we need to sum the leaf values of true paths to compute the final score. However, in the case of SumPath, given a leaf node's value, its associated SumPath value (either 0 or r), and $(+, \cdot)$ operations, there is no formula to express the logic: `SumPath == 0 ? leafValue : 0`. In the case of MultiplyPath, the logic `MultiplyPath == 1 ? leafValue : 0` can be expressed as formula `MultiplyPath * LeafValue`. However, this formula suffers a high computation overhead, because it requires as many (expensive) homomorphic multiplication operations as the length of each path.

Problem 2: Expensive Homomorphic Rotations. When we homomorphically compare a threshold and an input feature at each node, we run Figure 2 in a SIMD manner using a large number of ciphertext slots, and thus multiple comparison results get stored across multiple slots in the ciphertext. After, in order to prepare for computing SumPaths (or MultiplyPaths) based on these results, we need to clone as many ciphertexts as the number of unique (feature type, threshold value) pairs existing across all trees, each of which represents the associated node's comparison result, and rotate the ciphertext to align all comparison results to the 1st slot in the plaintext vector. We do this because FHE addition/multiplication operations are done element-wise on the same slot index. Due to this requirement of comparison value alignment, RCC-PDTE has to run as many homomorphic rotations as the number of unique (feature type, threshold value) pairs in all trees. And after computing SumPaths based on those slot-aligned ciphertexts, RCC-PDTE packs all those SumPath results within a single ciphertext for space efficiency, which again requires as many rotations as the number of tree paths. Such a problem of having to run many rotations aggravates in decision forests, because there are many such trees (e.g., 100 or even 1000) to compute.

Problem 3: Large Ciphertext Size. RCC-PDTE’s CW encoding requires a large ciphertext size due to its requirement of bit-wise encoding and encryption. In the case of 32-bit precision input features, RCC-PDTE requires a query ciphertext size of 85.7MB, in which case the majority of inference runtime occurs in the transmission of data over the network.

4. Our Protocol: SilentWood

In this section, we explain how SilentWood overcomes the limitations of RCC-PDTE to design efficient private evaluation of gradient boosting models (XGBoost and AdaBoost). SilentWood leverages RCC-PDTE’s number comparison (§3.1) and SumPath computation (§3.2) to evaluate multiple decision trees in a SIMD manner. Then, SilentWood efficiently computes the private inference result based on three novel techniques: blind code conversion, computation clustering, and ciphertext compression. Each of these techniques solve the three problems of RCC-PDTE (§3.3).

Threat Model: The server’s secret is the trained gradient boosting model. The client’s secret is its feature inputs for inference. At the end of the private inference protocol between the server and client, the server learns nothing about the client’s feature inputs, whereas the client learns only the following: (1) the inference score/probability of each classification; (2) the capped (i.e., maximum possible) number of trees and the capped total number of paths across all trees.

4.1. Blind Code Conversion

The problem of RCC-PDTE’s SumPath algorithm is that its outputs (i.e., 0 for a true path and a uniformly distributed random value for a false path) are arithmetically incompatible for homomorphic score aggregation of trees.

To solve this problem, SilentWood proposes a practical and light-weight two-party protocol: blind code conversion (BCC). In this protocol, the server sends its intermediate ciphertext to the client, who decrypts the ciphertext and manually modifies the plaintext values to make them arithmetically compatible with the server’s score aggregation. The BCC protocol is illustrated in Figure 6.

Figure 5 illustrates an example of private XGBoost score computation based on BCC, where the blind code conversion protocol between the server and client takes place in step 1. At a high level, the server runs the BCC protocol with the client to blindly convert the SumPath values of true paths (0) to 1, and the SumPath values of false paths (non-zero random number) to 0. At the end of the BCC protocol, the server homomorphically multiplies the resulting ciphertext to its RLWE plaintext that encodes an array of leaf values, where each plaintext slot (leaf value) matches its associated ciphertext slot (path). As a result, the leaf values for false paths get masked to 0, while the ones for true paths remain. In the end, the server aggregates all survived scores according to the class by rotating and adding the slot values in the ciphertext(s) to compute the final score for each class. Then, the server

Notations

V_k : A list of initial plaintext input elements: $\{v_1, \dots, v_k\}$

v_i : The i -th plaintext input element in V_k

\hat{V}_k : A list of converted plaintext input elements:
 $\{\hat{v}_1, \dots, \hat{v}_k\}$

U_m : The list of all possible unique values for
plaintext input elements: $\{u_1, \dots, u_m\}$

C : An input RLWE ciphertext (having total N slots)

C_p : A padded RLWE ciphertext (generated from C)

C_s : A shuffled RLWE ciphertext (generated from C_p)

C_c : A converted RLWE ciphertext (generated from C_s)

f_j : The fixed total frequency of element u_j in C_p

\hat{u}_j : The converted value of u_j

f'_j : The fixed total frequency of element \hat{u}_j in C_s

Protocol

IN : C whose first k slots sequentially store $\{v_1, \dots, v_k\}$

Server : 1. Given C , generate C_p where each $u_j \in U_m$ gets
fixed frequency f_j

2. Given C_p , generate C_s where all elements in C_p
are uniformly shuffled

S→C : $\{C_s\}$

Client : Create C_c where each $v_i \in V_k$ is converted into $\hat{v}_i \in \hat{V}_k$

C→S : $\{C_c\}$

OUT : C_c comprises randomly shuffled $\hat{u}_1, \dots, \hat{u}_m$,
where each $\hat{u}_j \in \hat{U}_m$ ’s total frequency is fixed to f'_j .
Also, some k slots in C_c store $\hat{v}_1, \dots, \hat{v}_k$

TABLE 1: The structure of the blind code conversion protocol

compactly packs all class scores into a single ciphertext and sends it to the client, who decrypts it and considers the class with the highest score as the inference answer. In case of binary classification, a single final score is returned to the client and whether this score is positive or negative indicates the classification result. Note that the client can skip the final transformation of the aggregated score(s) (e.g., sigmoid or softmax), because it is sufficient to analyze the magnitude of untransformed aggregate scores to answer the classification.

During code conversion, it is important for the privacy concern that both the client and the server learn nothing about the values encrypted in the intermediate ciphertext (e.g., SumPath results). For this purpose, the server pads and uniformly shuffles the slots of the intermediate ciphertext before sending it to the client.

Padding: The server pads additional encrypted values to the ciphertext so that the frequency distribution of each type of value in the ciphertext remains always constant (e.g., the number of zeros and the number of non-zero random numbers in case of XGBoost inference). To know the appropriate number of each type of elements to pad to the ciphertext, the server should have the prior knowledge of the total frequency distribution of the values stored in the ciphertext (although not knowing the actual plaintext values in each slot).

Shuffling: After padding, the server homomorphically shuffles the slot values to make their decrypted values appear uniformly

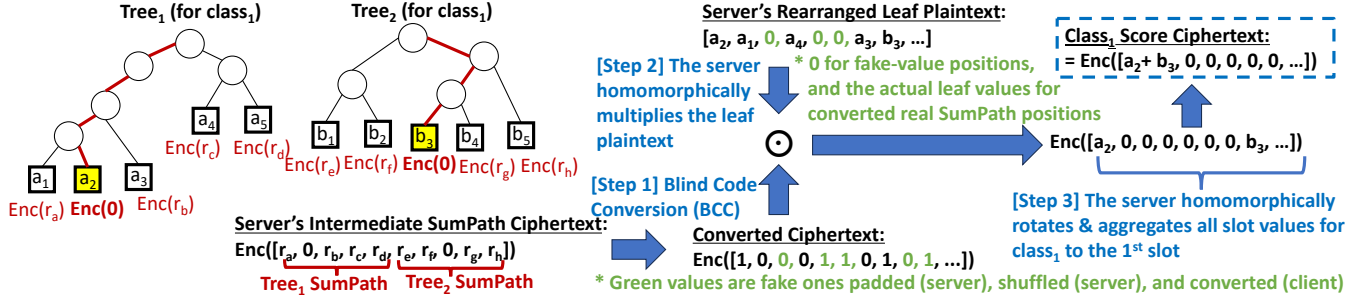


Figure 5: Private XGBoost score computation based on blind code conversion (BCC)

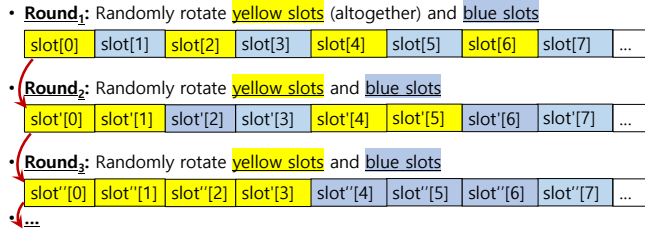


Figure 6: Illustration of blind shuffling

Algorithm 1 Blind Shuffling: Generating C_s based on C

- 1: **Input:** C
- 2: $C'_p \leftarrow \text{Pad } C$ with additional $\{u_1, \dots, u_m\}$ such that each $u_j \in U_m$ appears exactly f_j times, and the total elements after padding is the smallest power of 2 (say n)
- 3: $C_p \leftarrow \frac{N}{n}$ repetitions of C'_p 's padded n elements
- 4: **for** $s \in \{0, 1, \dots, \log_2(n) - 1\}$ **do**
- 5: $M_1 \leftarrow 2^s$ -gap mask plaintext # $[0, 0, \dots, 1, 1, \dots, 0, \dots]$ (with 2^s slots and 2^s slots)
- 6: $M_2 \leftarrow \text{Rotate}(M_1, 2^s)$ # s.t. $M_1 + M_2 = [1, \dots, 1]$ (N slots)
- 7: $P_1 \leftarrow C_p \odot M_1$ # cipher-plain multiplication
- 8: $P_2 \leftarrow C_p \odot M_2$ # s.t. $P_1 + P_2 = P$
- 9: $r_1 \leftarrow (\text{rand}() \cdot 2^s) \bmod n$
- 10: $r_2 \leftarrow (\text{rand}() \cdot 2^s) \bmod n$
- 11: **if** $((r_1 + r_2) \bmod 2^{s+1}) = 0$ **then**
- 12: $r_2 \leftarrow r_2 + 2^s$ # This ensures r_1 -slot-rotated elements
- 13: **end if** and r_2 -slot-rotated elements not to collide
- 14: $C_p \leftarrow \text{Rotate}(P_1, r_1) + \text{Rotate}(P_2, r_2)$ # shuffled
- 15: **end for**
- 16: $M_3 \leftarrow n$ -length mask plaintext # $[1, 1, \dots, 0, \dots]$ (n slots)
- 17: $C'_s \leftarrow C_p \odot M_3$
- 18: $C_s \leftarrow \text{pad } C'_s$ with $(N - n)$ uniformly shuffled $\{u_1, \dots, u_m\}$ such that each $u_j \in U_m$ appears f_m times
- 19: **Output:** C_s # a uniformly padded-and-shuffled C

randomly ordered. To efficiently shuffle the elements in the ciphertext, SilentWood designs the blind shuffling algorithm, which is visually illustrated in Figure 6.

Algorithm 1 is a detailed server-side logic that generates C_p and C_s based on C . Initially, the server homomorphically pads the input ciphertext C with additional u_1, \dots, u_m to the size of the nearest power of 2 (i.e., n) such that the ratio among u_1, \dots, u_m becomes fixed to f_1, \dots, f_n . Then,

the server further pads the ciphertext by $\frac{N}{n}$ repetitions of its contents to completely fill all slots, and generates C_p . Next, in each $(s + 1)$ -th shuffling round, the server rotates and shuffles the ciphertext C_p at the granularity of 2^s slots such that each chunk of 2^s consecutive elements gets rotated and shuffled together. Over each round, the size of this consecutive chunk gets doubled (as described in Figure 6). At the end of all shuffling rounds, the server trims the repeated slots (i.e., $n \sim (N - 1)$ indexes) and pad them with $N - n$ randomly ordered u_1, \dots, u_m such that each u_i 's total frequency in C_s gets fixed to f_i . Finally, C_s 's decrypted slots appear uniformly random to the client, having a randomly ordered u_1, \dots, u_m with a fixed frequency distribution.

In the case of XGBoost, the only information the client learns by decrypting C_s is that the total number of tree paths in the server's model is capped to some multiple of N (e.g., 16384 in case that RLWE's polynomial degree $N = 2^{14}$). On the other hand, the server knows the exact slot index of each SumPath value even after shuffling them (although not knowing their actual plaintext values), because it is the server who shuffled them. Therefore, the server can correctly generate the leaf value plaintext to homomorphically multiply to the converted ciphertext C_c for final score computation. Algorithm 1's required number of rotations is bound to $O(\log_2(\frac{N}{n}) + \log_2(n))$.

Extension to AdaBoost: Figure 5's XGBoost score computation can be transformed into AdaBoost score computation by replacing each leaf plaintext with $+\omega$ or $-\omega$, where the sign indicates the leaf's binary class label and ω is the weight of the tree it belongs to. As only the scalar values of the leaf plaintext need to be modified to turn the XGBoost into AdaBoost score computation, the total computation time and complexity is identical to that of the XGBoost protocol.

Comparing BCC to Programmable Bootstrapping: An alternative solution to BCC is the LWE-family scheme's programmable bootstrapping (PBS) [32], which enables the server to homomorphically convert encrypted plaintext values based on mapping information. Such PBS is computationally inefficient as the LWE scheme does not support SIMD operations. BCC overcomes such computational overhead at the cost of 1 RTT. In Table 2, we compare the features of BCC with PBS.

Comparing Blind Shuffling to Permutation Matrix: Multiplying a random permutation matrix [33] to the intermediate

	Regular PBS	SilentWood's BCC
Computation	Very heavy	Light
Communication	None	1 RTT
Plaintext	Each plaintext value can be converted into any other value	The same as regular PBS
Noises	The noise gets reset	The same as regular PBS
Security	The client & server learn nothing about the intermediate results	The client knows the maximum possible number of intermediate plaintext results (which is some multiple of N)
Constraints	None	The server needs knowledge on the frequency distribution of encrypted values (for padding)

TABLE 2: Comparing LWE-family FHE scheme's regular programmable bootstrapping (PBS) with SilentWood's BCC

ciphertext can give the same effect as random shuffling. However, homomorphic matrix-vector multiplications require $O(\sqrt{N})$ rotations and $O(N)$ multiplications [34], whereas SilentWood's blind shuffling requires $O(\log_2 N)$ rotations and $O(\log_2 N)$ multiplications.

BCC can be used not only in gradient boosting models, but also in other general FHE applications where the server has the prior knowledge of the frequency distribution of each type of values in the target ciphertext. We explain Algorithm 1 in detail with security analysis in §A.

4.2. Clustering Tree Nodes and Paths

The second limitation of RCC-PDTE is its high computation overhead due to a large number of homomorphic rotation operations required to compute and pack SumPath values. In private XGBoost inference, these two types of overhead also occurs before the server runs BCC with the client.

4.2.1. Node Clustering. To reduce the overhead of rotations, a straw-man solution is to compute comparison results only once for each distinct type of (feature, threshold) tree nodes across all trees in the model, and thereby eliminate redundant comparison operations. After, these results can be used as building blocks to create the desired combinations of edge values for each tree path in the model to compute all SumPath values. However, the benefit of this approach is limited, because this get will get the opportunity to eliminate comparison operations and rotations only for those nodes having exactly the same threshold values.

To more aggressively eliminate the number of computations, SilentWood clusters those nodes having not only the same threshold values, but also similar threshold values, and replaces their original threshold values to the average value of the nodes in the cluster. Figure 7a is an example of this approach: since node n_1 , n_3 and n_4 have the same feature type (stress) and similar thresholds (3.14, 3.12, 3.13), we cluster them, compute their average (3.13), and update their original threshold values with their average. Now that these 3 nodes have the same threshold values, their comparison results are the same, thus we only need to compute and rotate the comparison result only once for these 3 nodes instead of three times.

However, modifying their trained threshold values may degrade the model's inference accuracy. To mitigate the accuracy issue, upon updating the threshold values based of clustering, we verify the inference accuracy of the updated model with verification dataset. If the accuracy holds the

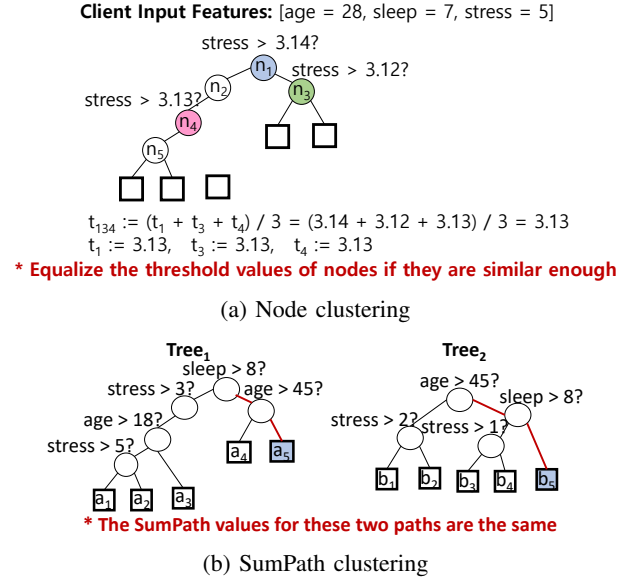


Figure 7: Techniques for computation clustering

same as before, we commit the update; otherwise, we abort the update. We repeat node clustering until there is no more updatable thresholds. This algorithm is described in 2. Given the clustering intensity is t , two nodes n_i and n_j get clustered if they are from the same feature type and their ratio of threshold difference is small enough satisfying: t (i.e., $\frac{|n_i.val - n_j.val|}{\text{MAX}(n_i.type) - \text{MIN}(n_i.type)}} < t$). The ideal intensity of node clustering depends on the characteristic of each dataset. Based on our experiments (Table 7), a generally ideal intensity was around 20% (i.e., $t = 0.2$). Note that even when the clustering intensity is big (i.e., aggressive clustering attempt), the accuracy drop is limited, because we validate the inference accuracy with verifying dataset and abort the update as needed. We have largely reduced the number of homomorphic computations (especially rotations) for tree nodes based on the node clustering technique.

4.2.2. Path Clustering. We further reduce the number of homomorphic computations by the path clustering technique. Figure 7b shows an illustrative example where path clustering is applicable: given the paths from 2 trees, path a_5 and path b_5 (shown as red lines) have the identical path condition: age > 45 and sleep > 8. This implies that their SumPath values will be the same, and thus the server only needs to encode one SumPath value instead of two during BCC. After, the

Algorithm 2 Clustering tree nodes

Input: \mathcal{N}, t # set of all distinct nodes, clustering intensity
do
 $isClustered \leftarrow \text{false}$
 for $n_i \in \mathcal{N}$ **do** # try clustering for each candidate node
 $\mathcal{C} \leftarrow \{n_i\}$
 for $n_j \in \mathcal{N} - \{n_i\}$ **do**
 if $n_i.type = n_j.type$ **then** # if same feature type
 if $\frac{|n_i.val - n_j.val|}{\text{MAX}(n_i.type) - \text{MIN}(n_i.type)} < t$ **then**
 $\mathcal{C} \leftarrow \mathcal{C} \cup n_j$ # cluster similar-threshold nodes
 end if
 end if
 end for
 if $|\mathcal{C}| > 1$ **then** # if 2 or more nodes are clustered
 $avg \leftarrow \frac{\sum_{n_k \in \mathcal{C}} n_k.val}{|\mathcal{C}|}$ # compute their average
 for $n_k \in \mathcal{C}$ **do**
 $n_k.val = avg$ # equalize the threshold values
 end for
 $isClustered \leftarrow \text{true}$
 end if
 end for
 while $isClustered$ # until no more clustering occurs
Output: \mathcal{N} # clustered final tree nodes

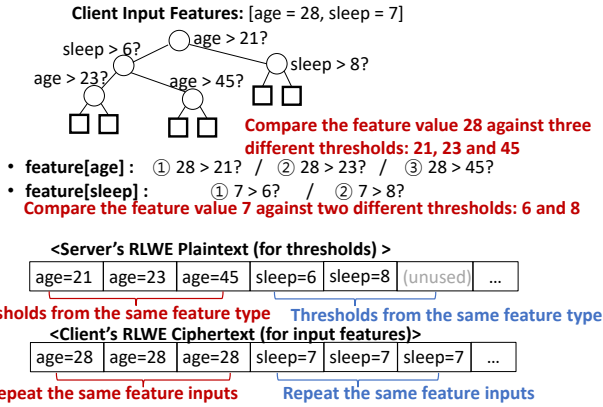


Figure 8: An example of repetitive data encoding

returned (converted) SumPath value can be used to compute the score for both a_5 and b_5 paths.

4.3. Ciphertext Compression

The third limitation of RCC-PDTE is the large communication cost due to bit-wise encryption required by CW-encoding, which increases the network overhead. In RCC-PDTE's protocol, the largest communication overhead occurs when the client sends the encrypted feature inputs to the server, which accounts for more than 95% of the total communication cost. Meanwhile, the overhead of the final ciphertext storing the server's inference result (and the BCC ciphertexts in case of SilentWood's gradient boosting protocol) account for less than 5%. Therefore, it is critical to reduce the size of the client-side initial query ciphertexts.

Algorithm 3 Ciphertext compression

Input: $dataArrList, dataInfoList, repetition$ # data array list, each data's start index and repetitive encoding gap
 $cDataArrList \leftarrow []$ # compressed array list
 $cDataArr \leftarrow []$ # compressed single array
 $dataArrCount \leftarrow 0$ # current data array count
 $cDataArrCount \leftarrow 0$ # current compressed array count
for $dataArr \in dataArrList$ **do** # compress all data
 $repeatCount \leftarrow dataArrCount \bmod repetition$
 for $\{data, info\} \in \{dataArr, dataInfoList\}$ **do**
 $targetIndex \leftarrow info.start + repeatCount \cdot info.gap$
 $cDataArr[targetIndex] \leftarrow data$
 end for
 $dataArrCount \leftarrow dataArrCount + 1$
 if $repeatCount = repetition$ **then**
 $cDataArrList.append(cDataArr)$
 $cDataArr \leftarrow []$
 end if
end for
 $encCDataArrList = []$
for $cDataArr \in cDataArrList$ **do** # encrypt all data
 $encCDataArr = \text{Encrypt}(\text{Encode}(cDataArr), sk)$
 $encCDataArrList.append(encCDataArr)$
end for
Output: $encCDataArrList$

Figure 8 is an example showing when repetitive data encoding is used in PDTE: the server's tree has 3 nodes conditioned on the *age* feature (whose each threshold is 21, 23, and 45), and 2 nodes conditioned on the *sleep* feature (whose each threshold is 6 and 8). The server homomorphically compares these threshold values against the client's encrypted $age=28$ and $sleep=7$ input feature values in a SIMD manner. Since the server has 3 distinct threshold values for *age* and 2 distinct threshold values for *sleep*, the client encodes its $age=28$ and $sleep=7$ values repetitively 3 times (capping to the server's maximum number of comparing the same feature type across all features). While such repetitive data encoding enables efficient SIMD comparison operation, such data repetition wastes the ciphertext space.

To resolve this issue, SilentWood designs the ciphertext compression protocol which works as follows: (1) the client removes repetitive data encoding before encryption and generates size-reduced compact ciphertexts; (2) once the server receives them, it homomorphically decompresses them by restoring the originally intended repetitions of data encoding. Figure 9 shows an example of ciphertext compression. In RCC-PDTE, when the client CW-encodes feature data, s/he has to create as many ciphertexts as the number of cw-encoded bits (M in this example), where each ciphertext repetitively encodes each feature's same bit 3 times (to help the server-side SIMD operation). On the other hand, using SilentWood's ciphertext compression, the client removes these repetitions of data before encrypting them, which results in 2 empty slots for each feature bit storage in the ciphertext. Therefore, the client can store the data's other digits' bits in this saved space. Applying this compact data encoding,

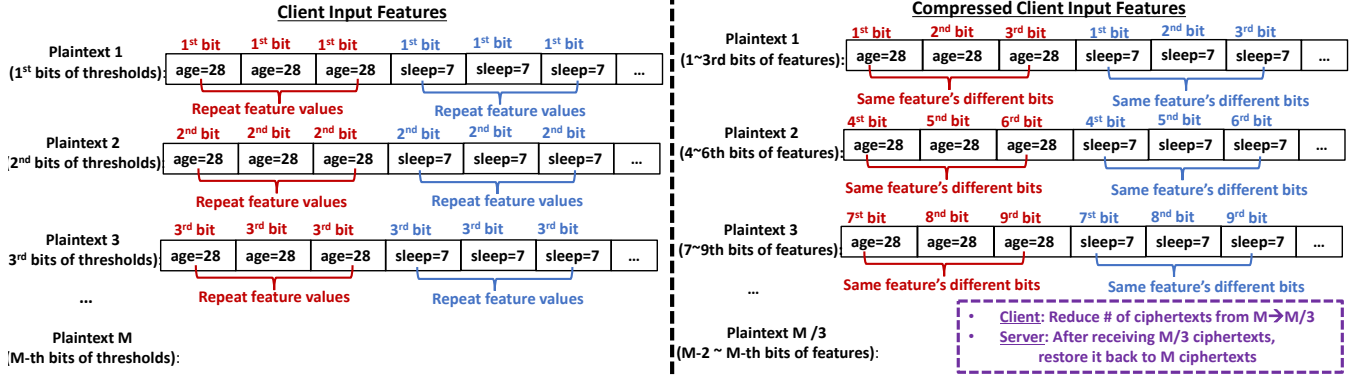


Figure 9: An example of ciphertext compression

the total required number of ciphertexts reduces from M to $\frac{M}{3}$. Once the server receives these compressed ciphertexts, it homomorphically performs the reverse operation of what the client did, effectively decompressing and restoring the originally intended data encoding format (i.e., 3 repetitions of feature bits).

Algorithm 3 generalizes the ciphertext compression algorithm, whose inputs are the following three: (1) a list of plaintext data vectors (*dataArrList*); (2) each data-specific encoding information (*dataInfoList*) which includes the start slot index (*.startIndex*) and the gap offset between each repetitive data encoding (*.gap*); and (3) the number of intended data repetition (*repetition*). One important requirement for the ciphertext compression algorithm is that all distinct data elements to be repeated at each round of repetition should have the same gap to their next round of data repetition, so that the server can restore the repetitions of all distinct data elements efficiently in a SIMD manner (e.g., the repetition of both the *age* and *sleep* feature data get recovered simultaneously).

SilentWood’s ciphertext compression is partially analogous to data compression algorithms (e.g., LZW). Our distinction is that regular compression algorithms often require the knowledge of plaintext data values (e.g., to create a token dictionary), whereas SilentWood’s ciphertext compression assumes only the format of repetitive data encoding is publicly known (e.g., gaps between repetitions, the total number of repetitions), while the actual data to be compressed is private.

Two-dimensional Slot Rotation: To further improve the efficiency of ciphertext compression, SilentWood uses both row-wise and column-wise slot rotation operations. In RLWE schemes, the first-half and the second-half plaintext slots in a ciphertext form an independent group of wrapping rotation, called row-wise rotation, which is used by RCC-PDTE. Meanwhile, column-wise rotation is an operation that 1-to-1 swaps the values in the 1st-half slots with those in the 2nd-half slots. Unlike RCC-PDTE that uses only the 1st-half slots with row-wise rotations, SilentWood fully utilizes all slots by using both row-wise and column-wise rotations during the client’s initial data encoding and the server’s node-wise comparison operations. During SumPath computation, the server performs column-wise rotations to align all comparison results to the 1st slot of the 1st-half slot group. This way,

SilentWood not only reduces the size of required ciphertexts into half, but also reduces the FHE computation time (because full utilization of slots saves the total number of ciphertexts engaged in comparison).

5. Evaluation

Implementation: We implemented SilentWood in C++ (5168 lines), which includes: the BCC protocol, computation clustering, ciphertext compression, and 2-dimensional rotation techniques. We also implemented our own version of SumPath algorithm based on depth-first search instead of RCC-PDTE’s breadth-first search to enhance memory efficiency. We implemented Python code (801 lines) that trains XGBoost models with node clustering. For FHE computation, we used the SEAL library [35] for the CPU version and the PhantomFHE library [36] for the GPU version.

Setup: We used i9-14900K 24-core CPU, 168GB RAM, and RTX 4900 GPU. To train and evaluate XGBoost, we used 13 UCI datasets [37], whose number of features, classes, and sample sizes are summarized in Table 3. For each dataset, we set the ratio of training, testing, and validation datasets as 0.6 : 0.2 : 0.2. We compared the performance of the three systems: XGBoost based on Zama’s Concrete ML [1], Baseline (RCC-PDTE with MultiplyPath), and SilentWood. The default number of trees was 100, the default maximum tree depth was 7, and the default intensity of node clustering was 0.2. We measured the inference time, inference accuracy, and ciphertext size. Additionally, we also conducted an ablation study by varying the default parameters and simulated various RTTs (50ms, 100ms, 200ms) with netem [38].

Summary of Results: In terms of computation time for inference, SilentWood is faster than Baseline by 28.1x and faster than Zama’s Concrete ML by 25.5x in case of using only CPU. When using GPU as well, SilentWood is faster than Baseline by 3.8x and faster than Zama’s Concrete ML by 122.2x. Compared to Baseline, SilentWood reduces the communication cost between the server and client down to 17.6% of the original size. Finally, when the RTT between the server and client is 50ms, SilentWood improves the end-to-end inference time by 4.7x even in the case of using GPU.

	Spam	Steel	Breast	Heart	Defect	Bank	PenDigits	Ailerons	Credit	Satellite	Elevators	Telescope	MFeat
Features	57	33	30	13	32	21	16	40	30	36	18	11	64
Classes	2	2	2	5	2	2	2	2	2	2	2	2	10
Samples	4,601	1,941	569	294	8,191	10,885	10,992	14,750	14,143	5,100	16,599	19,020	2,000

TABLE 3: Specification of benchmarks

Bench.	CPU version (SEAL Library)					GPU version (PhantomFHE Library)				
	Zama		Baseline		SilentWood	Zama		Baseline		SilentWood
	14-bit	16-bit	32-bit	16-bit	32-bit	14-bit	16-bit	32-bit	16-bit	32-bit
Spam	124.26s	109.71s	130.93s	4.30s	6.00s	72.46s	5.33s	5.78s	1.61s	1.82s
Steel	80.41s	28.65s	36.04s	0.97s	1.06s	61.91s	1.32s	1.69s	0.31s	0.35s
Breast	11.69s	21.20s	27.07s	0.75s	0.90s	10.30s	0.57s	0.96s	0.18s	0.19s
Heart	124.09s	57.50s	66.96s	1.41s	1.48s	82.90s	2.73s	3.16s	0.62s	0.63s
Defect	169.62s	239.73s	246.03s	5.34s	7.48s	82.74s	N/A	N/A	3.57s	3.86s
Bank	232.22s	315.91s	336.33s	8.85s	11.58s	118.64s	N/A	N/A	5.22s	5.54s
Pendigits	71.44s	46.98s	57.01s	1.60s	2.00s	52.96s	2.23s	2.63s	0.58s	0.69s
Ailerons	288.33s	270.76s	306.50s	9.04s	12.49s	129.88s	N/A	N/A	4.58s	5.01s
Credit	6.89s	10.23s	24.46s	0.84s	0.86s	5.50s	0.69s	0.90s	0.19s	0.19s
Satellite	16.79s	21.15s	31.68s	0.88s	1.21s	12.18s	1.12s	1.47s	0.28s	0.35s
Elevators	276.43s	322.89s	326.52s	9.55s	8.50s	133.29s	N/A	N/A	5.54s	5.09s
Telescope	181.88s	13.91s	19.44s	0.72s	0.93s	108.58s	0.57s	0.89s	0.12s	0.17s
MFeat	222.72s	91.82s	102.83s	3.38s	6.47s	231.42s	4.82s	5.41s	1.34s	1.61s
AVG.	93.35s	119.26s	131.68s	3.66s	4.69s	70.91s	2.15s	2.54s	0.58s	0.67s

(a) Computation time

CPU version			GPU version		
Zama	Baseline	SilentWood	Zama	Baseline	SilentWood
14-bit	16-bit	32-bit	14-bit	16-bit	32-bit
25.5x	32.5x	28.1x	122.2x	3.7x	3.8x

(b) SilentWood’s average speedup against Zama and Baseline

TABLE 4: Comparing computation time over various data bit-lengths (14 bits, 16 bits, and 32 bits), w/o GPU support (N/A denotes a GPU failure to handle the excessive memory requirement)

Bench.	Baseline				Baseline+B				Baseline+B+K				Baseline+B+K+C				Inference Accuracy			
	100T	200T	300T	400T	100T	200T	300T	400T	100T	200T	300T	400T	100T	200T	300T	400T	100T	200T	300T	400T
Spam	5.32s	5.33s	N/A	N/A	2.03s	2.92s	3.93s	4.87s	1.70s	2.43s	3.25s	4.32s	1.62s	2.32s	3.14s	4.21s	0.95	0.94	0.94	0.95
Steel	1.32s	2.16s	3.00s	3.55s	0.50s	0.79s	1.12s	1.30s	0.33s	0.47s	0.61s	0.66s	0.31s	0.45s	0.59s	0.64s	1.00	1.00	1.00	1.00
Breast	0.57s	1.09s	1.12s	1.12s	0.23s	0.46s	0.49s	0.51s	0.20s	0.25s	0.26s	0.28s	0.18s	0.22s	0.23s	0.25s	0.96	0.96	0.96	0.96
Heart	2.71s	4.36s	5.00s	5.87s	0.96s	1.58s	1.77s	2.05s	0.63s	1.24s	1.35s	1.19s	0.61s	1.21s	1.34s	1.18s	0.63	0.59	0.61	0.66
Defect	N/A	N/A	N/A	N/A	4.75s	7.08s	7.10s	N/A	3.58s	5.66s	7.58s	9.31s	3.57s	5.64s	7.53s	9.30s	0.79	0.81	0.80	0.81
Bank	N/A	N/A	N/A	N/A	6.20s	8.07s	N/A	N/A	5.32s	6.74s	8.76s	9.04s	5.23s	6.69s	8.68s	8.98s	0.79	0.80	0.79	0.79
Pendigits	2.22s	2.80s	3.23s	3.32s	0.78s	1.03s	1.19s	1.23s	0.60s	0.76s	0.84s	0.96s	0.57s	0.74s	0.82s	0.94s	0.99	1.00	1.00	0.99
Ailerons	3.33s	N/A	N/A	N/A	4.92s	4.95s	N/A	N/A	4.70s	7.52s	9.09s	11.13s	4.59s	7.46s	9.03s	11.01s	0.87	0.88	0.88	0.88
Credit	0.68s	0.87s	0.75s	1.09s	0.27s	0.35s	0.34s	0.50s	0.21s	0.21s	0.25s	0.25s	0.19s	0.18s	0.23s	0.23s	1.00	1.00	1.00	1.00
Satellite	1.11s	1.42s	1.61s	2.14s	0.41s	0.55s	0.62s	0.87s	0.30s	0.39s	0.41s	0.47s	0.27s	0.36s	0.38s	0.44s	0.99	0.99	0.99	0.99
Elevators	N/A	N/A	N/A	N/A	5.78s	5.77s	N/A	N/A	5.63s	8.99s	11.70s	13.87s	5.59s	8.93s	11.61s	13.88s	0.78	0.78	0.78	0.79
Telescope	0.56s	0.90s	1.24s	1.59s	0.22s	0.35s	0.50s	0.63s	0.13s	0.20s	0.20s	0.22s	0.11s	0.18s	0.18s	0.20s	1.00	1.00	1.00	1.00
MFeat	4.80s	7.04s	7.05s	N/A	1.77s	2.65s	3.13s	3.48s	1.42s	2.22s	2.70s	3.02s	1.34s	2.13s	2.60s	2.91s	0.91	0.93	0.93	0.94
AVG.	1.56s	1.94s	2.28s	2.67s	0.67s	1.00s	1.25s	1.50s	0.51s	0.74s	0.90s	1.04s	0.48s	0.71s	0.86s	1.01s	0.90	0.90	0.90	0.90

TABLE 5: Computation time over various numbers of trees (100, 200, 300 and 400) with GPU enabled

5.1. Aggregate FHE Computation Time

We evaluated the aggregate computation time (i.e., the server and client’s en/decoding, en/decryption, and homomorphic operations) for the cases where the feature and threshold bit sizes are 16 bits and 32 bits (quantized). The results are illustrated in Table 4. We tested only 14 bits for Zama’s Concrete ML, because its framework supports maximum 14-bit data length. We evaluated the cases with and without GPU. When using only CPU without GPU, Baseline’s average

computation time was 119.26s (16 bits) and 131.68s (32 bits), and Zama’s Concrete ML’s average time was 93.35s (14 bits), whereas SilentWood took 3.66s (16 bits) and 4.69s (32 bits). When using GPU, Baseline’s average computation time was 2.15s (16 bits) and 2.54s (32 bits), and Concrete ML’s average time was 70.91s (14 bits), whereas SilentWood’s average time was 0.58s (16 bits) and 0.67s (32 bits).

Bench.	Baseline				Baseline + B				Baseline + B + K				Baseline+ B + K + C				Inference Accuracy			
	7D	11D	15D	20D	7D	11D	15D	20D	7D	11D	15D	20D	7D	11D	15D	20D	7D	11D	15D	20D
Spam	5.32s	5.32s	7.28s	7.27s	2.03s	2.80s	2.68s	2.77s	1.70s	2.13s	2.32s	2.36s	1.62s	2.03s	2.23s	2.27s	0.95	0.94	0.94	0.94
Steel	1.31s	1.34s	1.31s	1.41s	0.50s	0.51s	0.50s	0.54s	0.33s	0.31s	0.32s	0.31s	0.31s	0.29s	0.30s	0.29s	1.00	1.00	1.00	1.00
Breast	0.57s	0.80s	0.80s	0.61s	0.23s	0.32s	0.31s	0.26s	0.20s	0.19s	0.22s	0.21s	0.18s	0.16s	0.19s	0.19s	0.96	0.96	0.96	0.96
Heart	2.73s	2.89s	2.86s	2.98s	0.96s	1.01s	0.99s	1.04s	0.63s	0.80s	0.79s	0.62s	0.61s	0.78s	0.77s	0.60s	0.63	0.63	0.63	0.63
Defect	N/A	N/A	N/A	N/A	4.75s	7.31s	N/A	N/A	3.59s	5.98s	7.95s	9.24s	3.57s	5.96s	7.93s	9.23s	0.79	0.80	0.81	0.81
Bank	N/A	N/A	N/A	N/A	6.17s	8.05s	8.39s	8.45s	5.32s	7.39s	7.18s	6.99s	5.23s	7.27s	7.09s	6.91s	0.79	0.80	0.80	0.80
Pendigits	2.22s	2.39s	2.33s	2.28s	0.78s	0.83s	0.81s	0.79s	0.60s	0.76s	0.70s	0.64s	0.57s	0.73s	0.67s	0.62s	0.99	0.99	0.99	1.00
Ailerons	N/A	N/A	N/A	N/A	4.92s	N/A	N/A	N/A	4.69s	8.34s	9.10s	9.77s	4.60s	8.26s	9.04s	9.65s	0.87	0.88	0.88	0.88
Credit	0.68s	0.77s	0.69s	0.65s	0.27s	0.30s	0.27s	0.26s	0.21s	0.19s	0.19s	0.19s	0.19s	0.16s	0.17s	0.17s	1.00	1.00	1.00	1.00
Satellite	1.11s	1.08s	1.14s	0.98s	0.41s	0.40s	0.42s	0.37s	0.30s	0.29s	0.24s	0.29s	0.27s	0.26s	0.21s	0.26s	0.99	0.99	0.99	0.99
Elevators	N/A	N/A	N/A	N/A	5.77s	N/A	N/A	N/A	5.64s	11.20s	13.47s	13.54s	5.58s	11.09s	13.42s	13.56s	0.78	0.80	0.80	0.80
Telescope	0.56s	0.60s	0.58s	0.57s	0.22s	0.24s	0.24s	0.23s	0.13s	0.13s	0.13s	0.13s	0.11s	0.11s	0.12s	0.12s	1.00	1.00	1.00	1.00
MFeat	4.81s	4.86s	4.85s	4.85s	1.77s	1.78s	1.77s	1.79s	1.41s	1.49s	1.44s	1.43s	1.34s	1.41s	1.37s	1.36s	0.91	0.92	0.93	0.92
AVG.	2.14s	2.23s	2.42s	2.40s	0.80s	0.91s	0.89s	0.89s	0.61s	0.70s	0.71s	0.69s	0.58s	0.66s	0.67s	0.65s	0.90	0.90	0.90	0.90

TABLE 6: Computation time over various maximum tree depths (7, 11, 15, 20) with GPU enabled

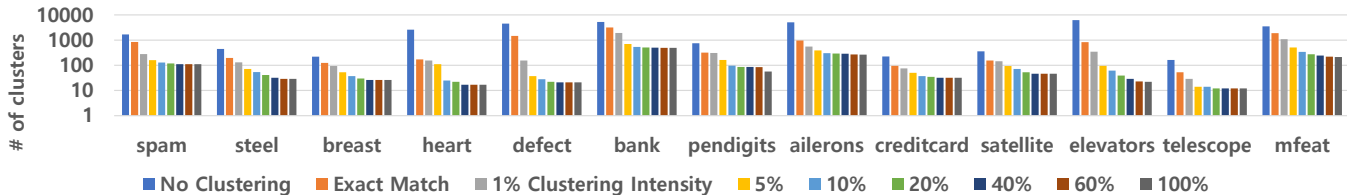


Figure 10: The number of node clusters across various node clustering intensities

	None	1%	5%	10%	20%	40%	60%	100%
Spam	0.94	0.93	0.92	0.92	0.92	0.91	0.91	0.91
Steel	1.00	1.00	1.00	1.00	1.00	1.00	1.00	1.00
Breast	0.69	0.69	0.66	0.64	0.66	0.64	0.59	0.59
Heart	0.74	0.8	0.81	0.81	0.81	0.81	0.81	0.81
Defect	0.82	0.82	0.82	0.82	0.8	0.81	0.81	0.81
Bank	0.99	0.99	0.99	0.99	0.99	0.99	0.99	0.99
PenDigits	1.00	1.00	0.99	0.99	0.99	0.99	0.99	0.99
Ailerons	0.88	0.88	0.88	0.88	0.88	0.88	0.88	0.88
Credit	1.00	1.00	1.00	1.00	1.00	1.00	1.00	1.00
Satellite	0.99	0.99	0.99	0.99	0.99	0.99	0.99	0.99
Elevators	0.8	0.8	0.81	0.82	0.8	0.81	0.81	0.81
Telescope	1.00	1.00	1.00	1.00	1.00	1.00	1.00	1.00
MFeat	0.94	0.93	0.92	0.92	0.90	0.90	0.90	0.90
AVG.	0.90	0.90	0.90	0.90	0.90	0.90	0.90	0.90

TABLE 7: Inference accuracy across node clustering intensities

5.2. Ablation Study over Various Tree Sizes

In Table 5, we varied the number of trees and evaluated the effectiveness of SilentWood’s each technique: Baseline plus BCC (denoted as Baseline + B), plus computation clustering (denoted as Baseline + B + K), and plus ciphertext compression (denoted as Baseline + B + K + C). We used GPU for these evaluations.

Given the tree size is fixed, using Baseline + B (0.8s, 1.05s) and Baseline + B + K (0.62s, 0.84s) contributed to additional speedup. BCC’s contribution was biggest for the computation speedup (2.32x on average), and computation clustering was next in place (1.35x). Meanwhile, ciphertext compression

Bench.	Path Clustering			BCC Runtime		
	Total Paths	Path Clusters	Overlapping Max. Paths	8-bit	16-bit	32-bit
Spam	1848	1787	5	110ms	116ms	120ms
Steel	538	342	13	55ms	61ms	60ms
Breast	239	134	42	27ms	29ms	29ms
Heart	1193	688	14	111ms	118ms	118ms
Defect	4287	4143	5	870ms	937ms	940ms
Bank	5222	5211	2	867ms	940ms	940ms
Pendigits	823	727	6	55ms	60ms	61ms
Ailerons	5249	5226	2	867ms	939ms	938ms
Credit	263	125	9	27ms	29ms	29ms
Satellite	459	363	6	27ms	31ms	30ms
Elevators	6395	6270	3	866ms	939ms	936ms
Telescope	239	34	30	27ms	29ms	29ms
MFeat	1586	1417	5	110ms	119ms	119ms
MEDIAN.	1193	727	6	55ms	60ms	60ms

TABLE 8: Efficiency of path clustering and BCC

also slightly sped up the computation time (1.06x), because it reduced the total number of ciphertexts engaged in FHE computation (although its benefit was limited due to GPU’s capability of large parallel computation).

Table 5 also shows the inference times across various number of trees (100 ~ 400). For all four candidate systems, the average computation time roughly linearly increased with the number of trees (since their number of rotations for handling SumPath linearly increased).

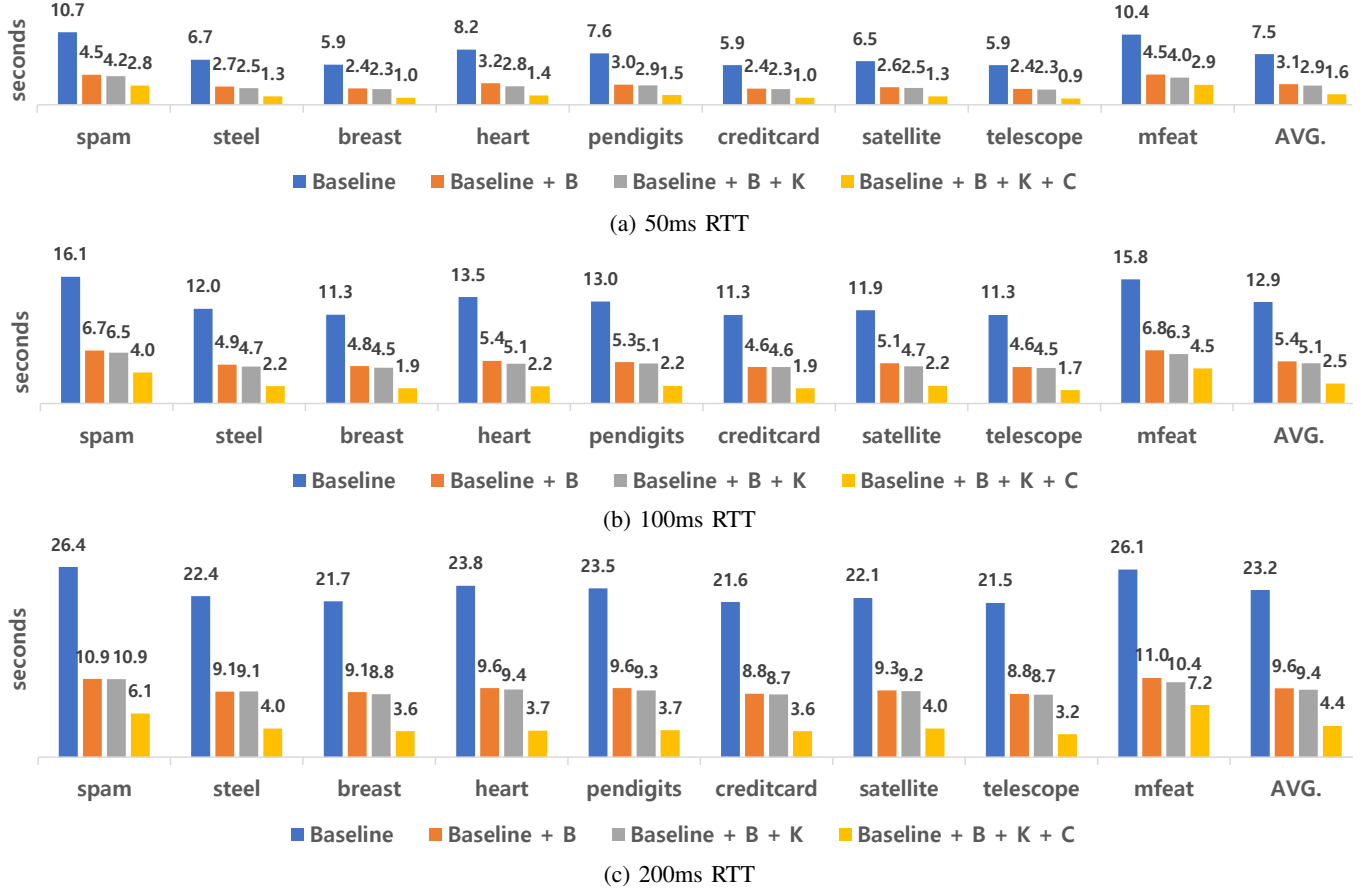


Figure 11: The end-to-end inference time between the server and client over various RTTs with GPU

Bench.	Baseline + B + K			Baseline + B + K + C		
	8-bit	16-bit	32-bit	8-bit	16-bit	32-bit
Spam	13.1MB	26.7MB	85.7MB	2.6MB	5.8MB	22.8MB
Steel	13.1MB	26.7MB	85.7MB	2.6MB	4.5MB	16.3MB
Breast	13.1MB	26.7MB	85.7MB	2.6MB	4.5MB	12.3MB
Heart	13.1MB	26.7MB	85.7MB	2.6MB	3.2MB	7.1MB
Defect	13.1MB	26.7MB	85.7MB	2.9MB	3.4MB	10.0MB
Bank	13.1MB	26.7MB	85.7MB	2.9MB	4.7MB	17.5MB
Pendigits	13.1MB	26.7MB	85.7MB	2.6MB	3.2MB	8.4MB
Ailerons	13.1MB	26.7MB	85.7MB	2.9MB	4.7MB	16.5MB
Credit	13.1MB	26.7MB	85.7MB	2.6MB	4.5MB	12.3MB
Satellite	13.1MB	46.4MB	85.7MB	2.6MB	4.5MB	16.3MB
Elevators	13.1MB	26.7MB	85.7MB	2.9MB	3.4MB	8.7MB
Telescope	13.1MB	26.7MB	85.7MB	2.6MB	3.2MB	5.8MB
MFeat	13.1MB	26.7MB	85.7MB	2.6MB	7.1MB	43.8MB
AVG.	13.00MB	29.79MB	85.75MB	2.70MB	4.34MB	15.12MB

TABLE 9: Communication cost (i.e., exchanged ciphertexts) between the server and client over various data bit-lengths

In Table 6, we measured the change in inference time across various maximum tree depths (7, 11, 15, 20). For all four candidate systems, the average computation time increased from depth 7 to 11, but it did not significantly change from 11 to 20. The reason was because the maximum depth of 11 was generally sufficient for trees to fully classify samples.

In the second-half columns of Table 5 and Table 6, we measured the trained XGBoost’s accuracy across various numbers of trees and maximum tree depths, where their average accuracy (0.9) stayed the same for all intensities.

5.3. Detailed Analysis of Each Technique

We more closely analyzed the effectiveness of SilentWood’s each of three techniques: node clustering, BCC, and ciphertext compression.

Node Clustering: Figure 10 shows the number of node clusters across various clustering intensity t (0% ~ 100%), where two nodes n_i and n_j get co-clustered if $\frac{|n_i.val - n_j.val|}{\text{MAX}(n_i.name) - \text{MIN}(n_i.name)} < t$. The success of clustering gradually decreased as we increased the intensity t . For example, when intensity $t = 0.2$, on average 2,388 nodes in XGBoost got clustered into 46 node clusters (i.e., $\frac{46}{2388} = 51.9x$ node reduction rate). While the bigger clustering intensity gave a higher opportunity of node clustering, the effectiveness of clustering (i.e., node reduction rate) did not increase anymore when t was greater than 0.4. Meanwhile, Table 7 shows that the inference accuracy was sustained even in high t values, because after each step of node clustering, we re-test the inference accuracy of the updated XGBoost model and abort the change if the accuracy changes.

Path Clustering: The first-half columns of Table 8 show the statistics of path clustering. The effectiveness of path clustering varied across benchmarks. The median total number of paths in XGBoost models was 1193, which were clustered into 727 distinct clusters. In other words, the median reduction rate of the number of homomorphic rotations for SumPath computation and packing was $\frac{1193}{727} = 1.64x$. In each benchmark, maximum 6 paths were identical in median (i.e., the paths having the same aggregate threshold conditions).

Blind Code Conversion: The second-half columns of Table 8 show the computation overhead of BCC. A majority of the overhead came from the rotation operations for blind shuffling. This overhead increased with the total number of unique tree paths in the model. The median computation time was 55ms \sim 60ms for 8-bit, 16-bit, and 32-bit data sizes.

Ciphertext Compression: Table 9 shows the total size of ciphertexts exchanged between the server and client during XGBoost inference. The ciphertext size increased with the feature data size. Without the compression technique, the size of ciphertexts was the same for Baseline + B + K, and Baseline + B + K + C, and their ciphertext sizes were constant regardless of the dataset. Specifically, the client’s number of ciphertexts for the initial query matched the number of CW-encoded data bits. For BCC and the final inference response, only a single ciphertext was needed, as all intermediate data fit in 16,382 slots of a single ciphertext. Using the 2-dimensional rotation, we could reduce the number of required ciphertexts roughly by half, and further reduced the ciphertexts by the factor of repetitive data encoding, where the repetition was calculated as dividing the total number of slots in a ciphertext by: the total number of feature types multiplied by the CW-encoded bit-length. On average, using ciphertext compression reduced the required ciphertext size from 85.75MB to 15.12MB in case of 32-bit feature data bit-length.

5.4. End-to-end Inference Time over Network

Figure 11 shows XGBoost’s end-to-end inference time for various RTTs. In case of 50ms RTT, SilentWood (1.6s) is 4.7x faster than Baseline (7.5s). The difference between Baseline + B + K (2.9s) and Baseline + B + K + C (1.6s) signifies the benefit of ciphertext compression reducing the network overhead.

6. Related Work

PDTE by Fully Homomorphic Encryption (FHE): XCOMP PDTE [39] and SortingHat [22] rotates polynomial coefficients in a polynomial ring to homomorphically compare encrypted values, but the algorithm is not scalable over data bit-length—their supported bit-length is only up to 11~13 bits. RCC-PDTE [20] proposes a more efficient comparison operator based on CW encoding. However, its SumPath computation is incompatible with score aggregation of decision forests, and also incurs much overhead both computation-wise and communication-wise when handling a large number of trees.

PDTE by Two-party Computation (2PC): 2PC is a special case of multi-party computation (MPC) where a server and

client compute the result of a common formula without revealing each other’s inputs to it. Brickell et al. [9] proposes an efficient constant-round protocol based on oblivious transfer (OT), garbled circuit (GC), and additive homomorphic encryption. Kiss et al. [13] combined them with other protocols to make an efficient PDTE protocol. However, 2PC usually incurs communication cost growing exponentially with the tree depth, because all tree paths need to be evaluated. Some of the later works addressed the issue of communication overhead by using oblivious RAM [15] or pseudo-random functions [16].

PDTE Extendable to Random Forest: HBDT [40] homomorphically trains a decision tree within a single security domain of an outsourced server. HBDT’s key idea is to represent all feature data with one-hot encoding to efficiently compare them against candidate threshold values during training. However, its one-hot encoding is not scalable over the data bit-length. For example, applying one-hot encoding to 32-bit feature input data requires 655,360 RLWE ciphertexts (around 19.7GB for $N = 2^{14}$ and $d = 2$), whereas SilentWood requires only around 5MB. BPDTE-CW [41] reduces the computation overhead of RCC-PDTE’s batch comparison (§3.1) by independently computing the comparison result for each tree node based on using only those CW-encoded digits whose values are 1 (instead of using all CW-encoded digits). However, this approach incurs a higher communication overhead (17.7% larger) than RCC-PDTE when the data bit-length increases from 11 bits to 16 bits. Also, since the majority of overhead (more than 85%) in PDTE comes from computing and packing SumPath values, the overall benefit of improving the speed of comparison operation is limited. Both HBDT [40] and BPDTE-CW [41], when generalizing their technique to a random forest setup, uses MultiplyPath (i.e., path conjugation) for path computation, incurring heavy cipher-cipher multiplications (see Baseline in §5.1), whereas SilentWood effectively bypasses this overhead by Sumpath with BCC.

Alouf et al. [7] proposes a private random forest scheme based on leveled homomorphic encryption [42] and threshold encryption, but it can support only a small number of trees (e.g., 3) with 8-bit data length. Ma et al. [8] proposes an MPC-based PDTE protocol using additive secret sharing, OT and GC, but it incurs $O(d)$ (d : tree depth) communication overhead and leaks the number of trees and depths. Wu et al. [11] proposes a scheme based on additive homomorphic encryption and OT, but its computation and communication cost is not scalable over the tree depth. Unlike all of these works, SilentWood’s computation and communication cost is less sensitive to the tree depth, only incurring the additional overhead of cipher-cipher additions, and does not leak the number of trees and depths.

Zama’s Concrete ML [1] is an FHE compiler based on TFHE and supports private inference of various ML models including XGBoost. However, TFHE is inefficient compared to RLWE-family schemes, because it does not support SIMD operation. Also, Concrete ML compiles a target algorithm into a bit-level logic circuit, thus even light addition operations get converted into heavy (bit-wise) homomorphic multiplications.

7. Conclusion

SilentWood provides private inference over gradient-boosting decision forests that significantly enhances performance over existing methods. SilentWood’s novel techniques are blind code conversion, computation clustering to duplicate homomorphic computations, and compressing ciphertexts to reduce the computation code. SilentWood achieves private XGBoost inference times up to 28.1× faster than the state-of-the-art baseline and up to 122.25× faster than Zama’s Concrete ML.

References

- [1] Zama, “Concrete ML,” 2024, <https://docs.zama.ai/concrete-ml>.
- [2] C. Gentry, “Fully homomorphic encryption using ideal lattices,” in *Proceedings of the 41st ACM Symposium on Theory of Computing*, 2009, pp. 169–178.
- [3] J. Fan and F. Vercauteren, “Somewhat practical fully homomorphic encryption,” *IACR Cryptology ePrint Archive*, p. 144, 2012.
- [4] A. C. Yao, “Protocols for secure computations (extended abstract),” in *Proceedings of the 23rd Symposium on Foundations of Computer Science*, 1982, pp. 160–164.
- [5] —, “How to generate and exchange secrets (extended abstract),” in *Proceedings of the 27th Annual Symposium on Foundations of Computer Science*, 1986, pp. 162–167.
- [6] G. Oded, *Foundations of Cryptography: Volume 2, Basic Applications*, 1st ed. USA: Cambridge University Press, 2009.
- [7] A. Aloufi, P. Hu, H. W. H. Wong, and S. S. M. Chow, “Blindfolded evaluation of random forests with multi-key homomorphic encryption,” *IEEE Transactions on Dependable and Secure Computing*, vol. 18, no. 4, pp. 1821–1835, 2021.
- [8] J. P. K. Ma, R. K. H. Tai, Y. Zhao, and S. S. M. Chow, “Let’s stride blindfolded in a forest: Sublinear multi-client decision trees evaluation,” in *Proceedings of the 28th Network and Distributed System Security Symposium*, 2021.
- [9] J. Brickell, D. E. Porter, V. Shmatikov, and E. Witchel, “Privacy-preserving remote diagnostics,” in *Proceedings of the 2007 ACM Conference on Computer and Communications Security*, 2007, pp. 498–507.
- [10] R. Bost, R. A. Popa, S. Tu, and S. Goldwasser, “Machine learning classification over encrypted data,” in *Proceedings of the 22nd Network and Distributed System Security Symposium*, 2015.
- [11] D. J. Wu, T. Feng, M. Naehrig, and K. E. Lauter, “Privately evaluating decision trees and random forests,” *Proceedings on Privacy Enhancing Technologies*, vol. 2016, no. 4, pp. 335–355, 2016.
- [12] R. K. H. Tai, J. P. K. Ma, Y. Zhao, and S. S. M. Chow, “Privacy-preserving decision trees evaluation via linear functions,” in *Proceedings of the 22nd European Symposium on Research in Computer Security*, 2017, pp. 494–512.
- [13] Á. Kiss, M. Naderpour, J. Liu, N. Asokan, and T. Schneider, “Sok: Modular and efficient private decision tree evaluation,” *Proceedings on Privacy Enhancing Technologies*, vol. 2019, no. 2, pp. 187–208, 2019.
- [14] M. Joye and F. Salehi, “Private yet efficient decision tree evaluation,” in *Proceedings of the 32nd IFIP Conference on Data and Applications Security and Privacy*, 2018, pp. 243–259.
- [15] A. Tueno, F. Kerschbaum, and S. Katzenbeisser, “Private evaluation of decision trees using sublinear cost,” *Proceedings on Privacy Enhancing Technologies*, vol. 2019, no. 1, pp. 266–286, 2019.
- [16] J. Bai, X. Song, S. Cui, E. Chang, and G. Russello, “Scalable private decision tree evaluation with sublinear communication,” in *Proceedings of the ACM Asia Conference on Computer and Communications*, 2022, pp. 843–857.
- [17] J. Bai, X. Song, X. Zhang, Q. Wang, S. Cui, E. Chang, and G. Russello, “Mostree: Malicious secure private decision tree evaluation with sublinear communication,” in *Proceedings of the Annual Computer Security Applications Conference*, 2023, pp. 799–813.
- [18] N. Cheng, N. Gupta, A. Mitrokovska, H. Morita, and K. Tozawa, “Constant-round private decision tree evaluation for secret shared data,” *Proceedings on Privacy Enhancing Technologies*, vol. 2024, no. 1, pp. 397–412, 2024.
- [19] J. Fu, K. Cheng, Y. Xia, A. Song, Q. Li, and Y. Shen, “Private decision tree evaluation with malicious security via function secret sharing,” in *Proceedings of the 29th European Symposium on Research in Computer Security*, 2024, pp. 310–330.
- [20] R. Akhavan Mahdavi, H. Ni, D. Linkov, and F. Kerschbaum, “Level up: Private non-interactive decision tree evaluation using levelled homomorphic encryption,” in *Proceedings of the 2023 ACM SIGSAC Conference on Computer and Communications Security*, ser. CCS ’23. New York, NY, USA: Association for Computing Machinery, 2023, p. 2945–2958. [Online]. Available: <https://doi.org/10.1145/3576915.3623095>
- [21] A. Tueno, Y. Boev, and F. Kerschbaum, “Non-interactive private decision tree evaluation,” in *Proceedings of the 34th IFIP Conference on Data and Applications Security and Privacy*, 2020, pp. 174–194.
- [22] K. Cong, D. Das, J. Park, and H. V. L. Pereira, “Sortinghat: Efficient private decision tree evaluation via homomorphic encryption and transciphering,” in *Proceedings of the 2022 ACM Conference on Computer and Communications Security*, 2022, pp. 563–577.
- [23] Kelong Cong and Jiayi Kang and Georgio Nicolas and Jeongeun Park, “Faster private decision tree evaluation for batched input from homomorphic encryption,” in *Proceedings of the 14th International Conference on Security and Cryptography for Networks*, 2024, pp. 3–23.
- [24] C. M. Bishop, *Pattern Recognition and Machine Learning (Information Science and Statistics)*. Berlin, Heidelberg: Springer-Verlag, 2006.
- [25] L. Breiman, “Random forests,” *Machine Learning*, p. 5, 2001.
- [26] J. H. Friedman, “Greedy function approximation: A gradient boosting machine,” *The Annals of Statistics*, vol. 29, no. 5, pp. 1189 – 1232, 2001. [Online]. Available: <https://doi.org/10.1214/aos/1013203451>
- [27] T. Chen and C. Guestrin, “XGBoost: A scalable tree boosting system,” in *Proceedings of the 22nd ACM SIGKDD International Conference on Knowledge Discovery and Data Mining*, ser. KDD ’16. New York, NY, USA: Association for Computing Machinery, 2016, p. 785–794. [Online]. Available: <https://doi.org/10.1145/2939672.2939785>
- [28] Y. Freund and R. E. Schapire, “A decision-theoretic generalization of on-line learning and an application to boosting,” in *Proceedings of the Second European Conference on Computational Learning Theory*, ser. EuroCOLT ’95. Berlin, Heidelberg: Springer-Verlag, 1995, p. 23–37.
- [29] C. Gentry, “A fully homomorphic encryption scheme,” Ph.D. dissertation, Stanford, CA, USA, 2009, aAI3382729.
- [30] J. Fan and F. Vercauteren, “Somewhat practical fully homomorphic encryption,” *Cryptology ePrint Archive*, 2012.
- [31] R. A. Mahdavi and F. Kerschbaum, “Constant-weight PIR: Single-round keyword PIR via constant-weight equality operators,” in *31st USENIX Security Symposium (USENIX Security 22)*. Boston, MA: USENIX Association, Aug. 2022, pp. 1723–1740. [Online]. Available: <https://www.usenix.org/conference/usenixsecurity22/presentation/mahdavi>
- [32] I. Chillotti, M. Joye, and P. Paillier, “Programmable bootstrapping enables efficient homomorphic inference of deep neural networks,” in *Cyber Security Cryptography and Machine Learning*, S. Dolev, O. Margalit, B. Pinkas, and A. Schwarzmann, Eds. Cham: Springer International Publishing, 2021, pp. 1–19.
- [33] Wikipedia, “Permutation matrix,” 2024, https://en.wikipedia.org/wiki/Permutation_matrix.
- [34] J. H. Cheon, K. Han, A. Kim, M. Kim, and Y. Song, “Bootstrapping for approximate homomorphic encryption,” in *Advances in Cryptology – EUROCRYPT 2018*, J. B. Nielsen and V. Rijmen, Eds. Cham: Springer International Publishing, 2018, pp. 360–384.

- [35] H. Chen, K. Laine, and R. Player, "Simple encrypted arithmetic library - seal v2.1," in *Financial Cryptography and Data Security*, M. Brenner, K. Rohloff, J. Bonneau, A. Miller, P. Y. Ryan, V. Teague, A. Bracciali, M. Sala, F. Pintore, and M. Jakobsson, Eds. Cham: Springer International Publishing, 2017, pp. 3–18.
- [36] H. Yang, S. Shen, W. Dai, L. Zhou, Z. Liu, and Y. Zhao, "Phantom: A cuda-accelerated word-wise homomorphic encryption library," *IEEE Transactions on Dependable and Secure Computing*, pp. 1–12, 2024.
- [37] Markelle Kelly, Rachel Longjohn, Kolby Nottingham, "The UCI Machine Learning Repository," 2024, <https://archive.ics.uci.edu>.
- [38] Michael Kerrisk, "Linux/UNIX system programming training," 2024, <https://man7.org/linux/man-pages/man8/tc-netem.8.html>.
- [39] W.-j. Lu, J.-j. Zhou, and J. Sakuma, "Non-interactive and output expressive private comparison from homomorphic encryption," in *Proceedings of the 2018 on Asia Conference on Computer and Communications Security*, ser. ASIACCS '18. New York, NY, USA: Association for Computing Machinery, 2018, p. 67–74. [Online]. Available: <https://doi.org/10.1145/3196494.3196503>
- [40] H. Shin, J. Choi, D. Lee, K. Kim, and Y. Lee, "Fully homomorphic training and inference on binary decision tree and random forest," in *Computer Security – ESORICS 2024: 29th European Symposium on Research in Computer Security, Bydgoszcz, Poland, September 16–20, 2024, Proceedings, Part III*. Berlin, Heidelberg: Springer-Verlag, 2024, p. 217–237. [Online]. Available: https://doi.org/10.1007/978-3-031-70896-1_11
- [41] K. Cong, J. Kang, G. Nicolas, and J. Park, "Faster private decision tree evaluation for batched input from homomorphic encryption," in *Security and Cryptography for Networks*, C. Galdi and D. H. Phan, Eds. Cham: Springer Nature Switzerland, 2024, pp. 3–23.
- [42] Z. Brakerski, C. Gentry, and V. Vaikuntanathan, "(leveled) fully homomorphic encryption without bootstrapping," in *Proceedings of the 3rd Innovations in Theoretical Computer Science Conference*, ser. ITCS '12. New York, NY, USA: Association for Computing Machinery, 2012, p. 309–325. [Online]. Available: <https://doi.org/10.1145/2090236.2090262>

Appendix A. Security Analysis: Blind Code Conversion

In this analysis, when we use the word ciphertext, this denotes an RLWE ciphertext. We also assume that each ciphertext contains total N (a power of 2) slots.

We define $Gen()$ as a black-box function that returns an array of length N comprising randomly ordered zeros and $rands$, such that the distribution ratio between the returned zeros and $rands$ is constant, c .

Definition 1. We regard a target function to be secure if the distribution of the array returned by a function appears to be indistinguishable from the distribution of the returned array of $Gen()$.

We define $EGS()$ as a blind shuffling function (i.e., Algorithm 1). The input to $EGS()$ is an encrypted array C having N slots, of which only the first k slots contain used elements. C 's decrypted array stores v_1, \dots, v_k in the first k slots. Whenever invoking $EGS()$, the frequency ratio of v_1, \dots, v_k (as decrypted forms) is not random, their order within the first k slots in C is also not random—we assume that these non-random characteristics depend on the caller's application status. We assume that the caller of $EGS()$ knows the distribution of v_1, \dots, v_k , but does not know their plaintext values (because they are encrypted). The internal logic of $EGS()$ is equivalent to Algorithm 1, detailed into the following four steps:

Step 1: (Line 2) Homomorphically pad ciphertext C 's first k elements to the smallest power of 2 elements, n (where $n < N$) such that the total frequency distribution of u_1, \dots, u_m becomes fixed as f_1, \dots, f_m at the end of the padding. The resulting ciphertext is C'_p .

Step 2: (Line 3) Create C_p which comprises $\frac{N}{n}$ sequential repetitions of the elements of C'_p .

Step 3: (Line 5 ~ 16) Homomorphically shuffle C_p such that the elements in C_p gets randomly re-ordered, with every n elements repeating their sequence. Specifically, the first n elements in the initial C_p get randomly re-ordered and stored between the 1st and n -th slots, and this randomized sequence of n elements repeats for total $\frac{N}{n}$ times throughout the N -length array. The resulting ciphertext is C_p .

Step 4: (Line 17 ~ 19) Keep only the first n encrypted slots in C_p , homomorphically mask the remaining $N - k$ slots to 0, and homomorphically pad these masked $N - n$ slots with a random sequence u_1, \dots, u_m , with their frequencies to be fixed to f_1, \dots, f_m . The resulting ciphertext is C_s .

We assume that the caller of the $EGS()$ has access to the entire internal logic of the above 4 steps.

Theorem 1. The distribution of the decryption of the array returned by $EGS()$ is indistinguishable from the distribution of the array returned by $Gen()$ (i.e., $EGS()$ is secure).

Proof. At a high level, if each of $EGS()$'s step 1~4 outputs its intermediate result as described above, then $EGS()$

is guaranteed to return a final array whose decryption is a mixture of u_1, \dots, u_m randomly ordered with the fixed frequencies f_1, \dots, f_m . In other words, the distribution of the (decrypted) array returned by $EGS()$ is indistinguishable from the distribution of the array returned by $Gen()$.

For the rest of this proof, we will explain how each step's internal FHE logic can be designed in order to make it return the intermediate result as described.

Step 1: Since we assume that the caller of $EGS()$ knows the ratio of these two types of inputs (although their actual values are unknown to the caller), the caller knows how many u_1, \dots, u_m are needed to force their frequency distribution to be fixed to f_1, \dots, f_m . The caller also knows how many of these values need to be padded to force the total number of elements in the array to be some power of 2 $n < N$. Specifically, the latter $N - n$ slots in C can be homomorphically masked to 0 (by generating an appropriate masking RLWE plaintext), and these slots can be added by the appropriate number of randomly ordered u_1, \dots, u_m (by generating an appropriate padding RLWE plaintext).

Step 2: C_p can be generated in total $\log \frac{N}{n}$ rounds, where each i -th round homomorphically rotates C'_p to the right by n^i slots to generate Q' and then homomorphically compute $C_p \leftarrow C_p + C'_p$ and $C'_p \leftarrow C_p$.

Step 3: Suppose that we label the first n slots in C_p with a base-2 index comprising $L = \log n$ bits. We run the for-loop total L rounds, where in each l -th round, we create two sparsely masked ciphertexts P_1 and P_2 where each ciphertext is created by zero-masking ciphertext C_p by the zeroing the slots

with sparsity gap size 2^{l-1} (e.g., $\overbrace{1111 \dots 0000 \dots 1111 \dots}^{2^{l-1} \quad 2^{l-1} \quad 2^{l-1}}$). Further, P_1 and P_2 should be exactly out of phase to each other, such that $P = P_1 + P_2$ (see Figure 6). Then, we randomly homomorphically rotate each ciphertext with the step size 2^{l-1} and merge back. After random rotations of P_1 and P_2 , we ensure that their rotated results still stay out-of-phase: if not, we further homomorphically rotate the rotated P_2 to the right by 1 additional step size (2^{l-1}). We continue these for total L rounds.

Now, we will prove why the above L -round shuffling procedure ensures full random ordering of the first n elements of C_p . Let's first consider the element stored at slot index i in the initial C_p . Notice that index i is a base-2 number comprising L bits denoted as i_L, i_{L-1}, \dots, i_1 (where each $i_k \in \{0, 1\}$). We further denote $[i_L i_{L-1} \dots i_l i_{l-1} \dots i_1]$ as the initial element stored at slot index i in P before starting any round of shuffling. We further denote \bar{i}_k as a negation of bit i_k , and denote $*_k$ as a wildcard for the k -th bit (i.e., can be either 1 or 0). Given these notations, notice that in each l -th round, $[i_L i_{L-1} \dots i_{l-1} i_{l-1} \dots i_1]$ (i.e., the element stored at slot index i in the initial P) gets a randomized distance to elements $[*_L *_L \dots \bar{i}_l *_l \dots *_1]$, whereas its distance to the elements $[*_L *_L \dots i_l *_l \dots \hat{i}_1]$ does not change. This implies that after the end of all $1, 2, \dots, L$ rounds of shuffling, element $[i_L i_{L-1} \dots i_l i_{l-1} \dots i_1]$ gets a randomized distance to all the other elements stored within

slot index $0, 1, \dots, n - 1$. And this is true for any other elements within slot index $0, 1, \dots, n - 1$. Therefore, all initial elements stored within slot index $0, 1, \dots, n - 1$ gets uniformly randomly repositioned among them after L rounds of shuffling. Meanwhile, the randomized sequence of the first n elements in the fully shuffled C_p repeats its sequence for $\frac{N}{n}$ times, because the initial C_p had $\frac{N}{n}$ repetitions of the first n elements in C'_p . Therefore, the final state of C_p is exactly what we expect as the result at the end of step 3.

Step 4: C_s can be generated in the similar manner as step 1 where we masked and replaced the latter $N - n$ elements of a ciphertext.

□